IRSTI 29.19.24; 29.19.31 https://doi.org/10.26577/ijmph.20261715

ELECTRONIC STATES IN ZnO/porousZnSe/ZnSe HETEROSTRUCTURES

A. Dyadenchuk [1], **R. Oleksenko** [2] **and E. Filipovich** [1]

[1] *Dmytro Motornyi Tavria State Agrotechnological University, Melitopol, Ukraine*

[2] *Volodymyr Vynnychenko Central Ukrainian State University, Kropyvnytskyi, Ukraine*

Email: roman.xdsl@ukr.net

(Received 5 January 2026; revised 12 May 2026; accepted 26 May 2026)

Abstract. ZnO nanowires have attracted considerable attention due to their wide band gap, high chemical stability, and pronounced quantumscale effects, making them promising components for optoelectronic and sensor devices. The electronic states of such nanostructures strongly depend on the properties of the substrate, especially in heterostructures containing porous materials. In this work, the formation of quantum levels and the electronic properties of ZnO nanowires in two systems ZnO/ZnSe(bulk) and ZnO/porousZnSe/ZnSe with porosity ranging from 20% to 80% were theoretically investigated. The base nanowire model, with a radius of 25nm and a height of 500nm, describes the structure as a cylindrical infinite potential well, while the influence of porous ZnSe is incorporated through porositydependent barrier parameters: dielectric constant, and electron affinity. Analytical solutions of the Schrödinger equation obtained using Bessel functions, together with numerical simulations in Matlab, revealed strong radial quantum confinement: the radial quantization energy significantly exceeds the longitudinal one for the first levels, and the groundstate energy is about 0.0015eV. To quantitatively analyze the effect of substrate porosity, a finite cylindrical potential well model is employed, in which the barrier height $V_0(P) = \chi_{ZnO} - \chi_{eff}(P)$ explicitly depends on porosity through the dielectric constant and electron affinity of porous ZnSe, calculated using the Bruggeman effective medium equation and the Penn relation, respectively. Numerical simulations performed for nanowire radii in the range $5-20$ nm showed that increasing ZnSe porosity leads to systematic upward shifts of the ground-state energy, with absolute changes reaching up to $3-4$ meV for nanowires with radius $R < 10$ nm. The obtained results confirm that porous ZnSe is an effective tool for tuning the electronic states of ZnO nanowires and open up opportunities for optimizing UV photodetectors and photovoltaic converters by controlling substrate porosity.

Keywords: ZnO nanowires, porous ZnSe, quantum confinement, electronic states, optoelectronic applications.

INTRODUCTION

ZnO nanowires have attracted considerable attention due to their wide band gap, high stability, and pronounced quantumscale effects, which make them promising for optoelectronic and sensor applications [1, 2, 3]. It is well established that the electronic states of nanowires strongly depend on the properties of the substrate, particularly on the electron affinity, dielectric constant, and potential barrier at the heterostructure interface [4, 5]. The combination of a porous substrate with ZnO nanowires is of special interest, as their parameters can be tuned by adjusting the porosity [6]. The emergence of porous ZnSe as a new type of substrate [7, 8] has introduced an important scientific challenge-namely, the lack of comprehensive theoretical studies on its influence on the quantum levels of ZnO nanowires. This gap highlights the relevance of the present work, since the ability to control energy states through substrate modification is crucial for optimizing UV photodetectors, sensors, and other nanophotonic devices.

The theoretical significance of this study lies in modeling the electronic states of ZnO nanowires while accounting for the porositydependent parameters of ZnSe. The practical value is associated with the possibility of deliberate tuning of the electronic and optical properties of such heterostructures for modern optoelectronic applications.

Based on previous studies of systems, such as ZnO/porous-Si and ZnO/porous-GaN, in which the main focus was on morphological and optical effects, this work shows for the first time

the effect of the porosity of ZnSe itself on the barrier parameters and quantum states of ZnO nanowires.

Literature review

ZnO nanostructures are actively studied due to their unique electronic and optical properties, which determine their prospects for optoelectronic and sensor applications [9, 10, 11]. A separate direction of modern research is associated with the growth of ZnO nanostructures on porous semiconductor substrates, which are able to change the interface properties, refractive index and local electric fields [12, 13, 14]. The combination of ZnO and porous Si is extremely effective [15, 16]. The porous structure reduces the effective refractive index, reduces optical losses and improves light absorption, which is critically important for photodetectors and photoconverters [17, 18, 19, 20]. The authors of the works [19, 21] found that in the ZnO/porous-Si and ZnO/porous-GaN systems, porosity affects the growth morphology and optical response, confirming the ability of porous substrates to significantly modify the properties of the superimposed nanostructures. It should be emphasized that the results obtained for ZnO/porousSi systems cannot be directly transferred to ZnO/porousZnSe due to differences in electron affinity, dielectric permittivity, and band alignment.

A special place among ZnO nanostructures belongs to nanowires. Their one-dimensional geometry provides strong quantum-scale effects, high surface area and directional transport of charge carriers [22, 23, 24]. Such properties make nanowires much more sensitive to changes in the interface and substrate parameters than films or nanoparticles, which allows a more complete assessment of the influence of porous materials on the electronic states of ZnO. Thus, it has been established that the radius of the nanowire determines the position and density of discrete energy levels formed as a result of radial quantum confinement [25]. However, most of the work focuses on morphological and photoluminescent effects, but the influence of porosity on the electronic parameters of the barrier layer and quantum levels of nanowires remains insufficiently studied. Porous ZnSe has recently attracted particular attention [26, 27, 28] due to its tunable optical and electronic behavior, chemical stability, and potential for processing [29, 30]. Porous ZnSe has an energy alignment compatible with ZnO and can significantly change the electron affinity, permittivity, and effective mass. For example, we previously investigated the formation of ZnO nanowire arrays on porous ZnSe obtained by electrochemical etching [31], and analyzed their morphology, crystal structure, and luminescent properties that determine the photosensitivity of the created phototransducer. The present theoretical model was developed to complement the experimental study reported in [31], where ZnO nanowire arrays on porous ZnSe were synthesized and characterized. While [31] focused on morphological properties, the present work provides the first theoretical framework describing how ZnSe porosity modifies the potential barrier and quantum energy levels of the nanowires, thereby offering a quantitative basis for interpreting the experimentally observed porosity-dependent optical response.

Thus, despite significant progress in the study of ZnO nanowires and porous substrates, the influence of ZnSe porosity on the formation of the energy spectrum of ZnO nanowires remains insufficiently explored. This gap in understanding defines the scientific novelty and relevance of the present work.

Modeling electronic states in a nanowire ZnO/porous-ZnSe/ZnSe

To describe the electronic states in a ZnO nanowire, a cylindrical region of radius R and height H is considered, which corresponds to the real geometry of nanowires grown on porous ZnSe. The porous structure of ZnSe provides a vertical growth direction and the formation of an array of nanowires with similar geometric parameters. The model assumes that the nanowire has impermeable walls (infinite potential well), which is a standard approximation for ZnO nanostructures with a high potential differ-

ence at the ZnO/ZnSe interface.

The region of electron motion is described by cylindrical coordinates (r, θ, z):

$$0 \le r \le R, \qquad 0 \le \theta \le 2\pi, \qquad 0 \le z \le H.$$

The stationary states of an electron are described by the Schrödinger equation [32]:

$$-\frac{\hbar^2}{2m^*}\nabla^2\psi = E\psi,$$

where m^* is the effective mass of an electron in ZnO ($m^* = 0.24m_0$).

In cylindrical coordinates, the Laplace operator has the form [33]:

$$\nabla^2\psi = \frac{1}{r}\frac{\partial}{\partial r}\left(r\frac{\partial\psi}{\partial r}\right) + \frac{1}{r^2}\frac{\partial^2\psi}{\partial\theta^2} + \frac{\partial^2\psi}{\partial z^2}.$$

To solve the equation, the separation of variables method is used:

$$\psi(r,\theta,z) = R(r)\,\Theta(\theta)\,Z(z).$$

Substituting this representation into the Schrödinger equation leads to the radial differential equation:

$$r^2\frac{d^2R}{dr^2} + r\frac{dR}{dr} + (k_r^2r^2 - m^2)R = 0,$$

where $R(r)$ is the radial part of the wave function, m is the azimuthal quantum number, k_r is the radial component of the wave number.

The solution is the Bessel function of the first kind [34]:

$$R(r) = J_m(k_r r).$$

The boundary condition on the nanowire wall is

$$\psi(R,\theta,z) = 0 \quad \Rightarrow \quad J_m(k_r R) = 0.$$

Since Bessel functions have discrete zeros x_{m,n_r}, we obtain:

$$k_r = \frac{x_{m,n_r}}{R}.$$

Thus, the radial quantization in a nanowire is determined by the geometry of the structure and the properties of the Bessel functions.

The angular part satisfies:

$$\frac{d^2\Theta}{d\theta^2} + m^2\Theta = 0,$$

with harmonic solutions:

$$\Theta(\theta) = \cos(m\theta), \qquad m = 0,1,2,\ldots$$

Along the z axis, the electron moves in a onedimensional infinite quantum well with boundary conditions:

$$Z(0) = 0, \qquad Z(H) = 0.$$

The solution is a standing wave:

$$Z(z) = \sin\left(\frac{n_z\pi z}{H}\right), \qquad n_z = 1,2,3,\ldots$$

The corresponding energy eigenvalues for motion along the axis are:

$$E_z = \frac{\hbar^2}{2m^*}\left(\frac{n_z\pi}{H}\right)^2.$$

Since $H \gg R$, the longitudinal quantization is weak.

The full expression for the energy levels of an electron in a cylindrical nanowire is:

$$E_{m,n_r,n_z} = \frac{\hbar^2}{2m^*}\left[\left(\frac{x_{m,n_r}}{R}\right)^2 + \left(\frac{n_z\pi}{H}\right)^2\right],$$

where m is the azimuthal quantum number, n_r is the zero number of the Bessel function $J_m(x)$, n_z is the quantum number along the axis, and R and H are the radius and height of the nanowire.

Numerical implementation of the model

Analytical expressions for the wave functions and energy levels were used as a basis for numerical simulations performed in the Matlab environment. For radial quantization, tabulated values of the first zeros x_{m,n_r} of the Bessel functions $J_m(x)$ were used. For each triple of quantum numbers (m, n_r, n_z), the radial component of the energy (determined by the zero of the Bessel function), the longitudinal component (which depends on the height of the nanowire), and the total energy in electron volts were calculated.

Based on the analytical expression for the wave function

$$\psi(r,\theta,z) = J_m\left(\frac{x_{m,n_r}}{R}\,r\right)\cos(m\theta)\,\sin\left(\frac{n_z\pi z}{H}\right),$$

the probability density $|\psi(r,\theta,z)|^2$ is calculated.

Materials and Methods

Within the framework of the study, several interconnected stages were sequentially implemented, aimed at determining the influence of the porous ZnSe layer on the electronic states of ZnO nanowires. At the first stage, a quantum-mechanical model of the nanowire was formulated, which is described as a cylindrical infinite potential well, taking into account the real geometric parameters of the structure. At the next stage, the porosity of ZnSe was integrated into the model through the finite cylindrical well framework, in which the barrier height $V_0(P)$ depends on porosity via the effective dielectric constant and electron affinity of porous ZnSe, calculated using the Bruggeman effective medium equation and the Penn relation, respectively, which provided the opportunity to evaluate the change in the potential profile at the ZnO/ZnSe interface. To illustrate the geometry of the model, a diagram (Fig. 1) was used, which demonstrates the spatial configuration of ZnO nanowires on a ZnSe substrate.

The numerical implementation of the model was carried out in the Matlab environment, where the energy levels, probability density, and their dependence on porosity were calculated for a wide range of quantum numbers and geometric parameters.

Such a comprehensive approach allowed us to establish the regularities of the influence of porosity on quantum states in ZnO nanowires and to determine the possibilities of targeted control of their electronic properties.

Results and Discussion

Numerical simulation of electronic states in a ZnO nanowire with a radius of 25 nm and a height of 500 nm showed that the energy spectrum has a pronounced anisotropic structure, due to the large ratio $H/R = 20$. Radial quantization is much stronger than longitudinal, which leads to the dominance of the radial component of energy. Analysis of the first ten lowest levels (Table 1) shows that the radial component of the energy E_r exceeds the longitudinal E_z by two to three orders of magnitude, and a change in the quantum number n_z has practically no effect on the total energy. On the other hand, a transition to the next radial zero or an increase in the azimuthal number leads to a significant increase in the energy level. The ground state $(0,1,1)$ has an energy of about 0.0015 eV, which corresponds to weak quantum confinement along the axis and strong confinement in the transverse direction. Thus, the spectrum of the nanowire is quasi-continuous along the axis and discrete in the radial direction, which is a typical feature of tall nanostructures with a small radius.

Fig. 2 shows the distribution of $|\psi|^2$ for the states $(0,1,1)$, $(0,1,2)$ and $(1,1,1)$ in three sections: the transverse section at $z = H/2$ and two longitudinal sections at $y = 0$ and $x = 0$.

The state $(0,1,1)$ with energy E=0.0015 eV corresponds to the ground quantum level. In the cross-section a circular symmetry of the distribution is observed, which is due to the absence of angular dependence at $m = 0$. The probability density has a maximum in the center of the nanowire. In the longitudinal sections, one half-wave is visible along the z-axis, which is consistent with the quantum number $n_z = 1$. This form of the wave function indicates the localization of

Table 1 – Energy levels of an electron in a nanowire

	State	E (eV)	E_r/E_z
1	$(0,1,1)$	0.001475	234.4
2	$(0,1,2)$	0.001494	58.6
3	$(0,1,3)$	0.001525	26.0
4	$(1,1,1)$	0.003735	595.0
5	$(1,1,2)$	0.003754	148.8
6	$(1,1,3)$	0.003786	66.1
7	$(2,1,1)$	0.006705	1068.9
8	$(2,1,2)$	0.006724	267.2
9	$(2,1,3)$	0.006755	118.8
10	$(0,2,1)$	0.007746	1235.0

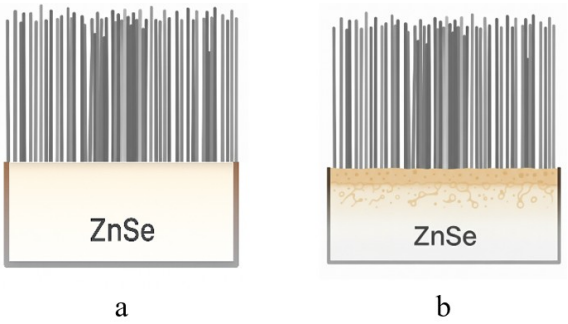

Figure 1 - Schematic representation of ZnO/ZnSe heterostructures: a) nanowires ZnO on bulk-ZnSe; b) nanowires ZnO on porous-ZnSe.

the electron in the volume of the structure and weak quantum confinement along the axis.

For the state $(0,1,2)$ with the same energy value, but with $n_z = 2$, the spatial distribution changes. In the longitudinal sections, two maxima are observed along the z-axis, which corresponds to the second mode of longitudinal quantization. The cross-section at the level $z = H/2$ exhibits the minimum probability density, since in this plane the wave function has a node. The radial distribution remains unchanged, which confirms the independence of the radial localization from n_z for fixed m and n_r.

The state $(1,1,1)$ with energy E=0.0037 eV demonstrates the influence of the angular quantum number $m = 1$. In the cross-section, a two-hump structure is observed with maxima along the x-axis and a node along the y-axis, which corresponds to the angular dependence $\cos\theta$. In the $y = 0$ plane, the probability density is maximum, while in the $x = 0$ plane it goes to zero, confirming the presence of a nodal surface. The longitudinal distribution preserves one half-wave in z, similar to the state $(0,1,1)$. From the point of view of photovoltaic applications, the obtained energy level structure is of significant importance. The quasi-continuous spectrum along the nanowire axis forms an increased density of states, which contributes to the effective absorption of photons and the generation of charge carriers. According to the fundamental model of S. Sze [35], 1D structures have a specific density of states, which, as shown in the works of Arbiol et al. [36], ensures the effective generation of carriers through the quasi-continuous axial spectrum. Discrete radial levels determine the spectral selectivity of absorption and spatial localization of electrons, while the shape of the wave functions directly affects the features of the transport of carriers along the nanowire [37]. The obtained modeling results indicate that ZnO nanowires on porous ZnSe are promising components of UV photodetectors and solar converters, as they combine strong quantum confinement in the transverse direction with efficient carrier transport along the axis.

The influence of substrate porosity on the electronic states of the ZnO nanowire arises from porosityinduced modifications of the interfacial electrostatic environment. Increasing ZnSe porosity reduces the effective dielectric constant and changes the electron affinity and barrier height at the ZnO/ZnSe interface. These combined factors alter the boundary conditions for the confined carriers and lead to the observed shifts in the quantized energy levels.

The use of an infinite potential well is justified by the large conduction band offset at the ZnO/ZnSe interface (1.0–1.2 eV), which significantly exceeds the quantization energies obtained for the considered nanowire radii. Under these conditions, the penetration of the electron wave function into the ZnSe matrix is negligible, and the confinement is effectively determined by the ZnO region. As a result, the infinite-well approximation provides an accurate description of the quantized states while allowing for analytical treatment of the model.

Finite potential barrier and porosity-dependent parameters

The considered model above of the infinite well used describes the idealized case where the wave function is completely localized in the middle of the ZnO nanowire. However, in the real structure of ZnO/porous-ZnSe/ZnSe, the barrier between the nanowire and the substrate is a skin and the difference in the electron affinities of the materials. Since the porosity of ZnSe changes its electron affinities, the barrier height is a function of the porosity P. Therefore, to correctly describe the effect of porosity at the quantum levels, the finite cylindrical well model is used.

The porous ZnSe layer is considered as a two-phase effective medium consisting of the crystalline phase of ZnSe and pores filled with air. The effective permittivity $\varepsilon_{\text{eff}}(P)$ was determined using the Bruggeman approximation [38]:

$$P\,\frac{\varepsilon_{\text{void}}-\varepsilon_{\text{eff}}(P)}{\varepsilon_{\text{void}}+2\varepsilon_{\text{eff}}(P)}+(1-P)\,\frac{\varepsilon_{\text{ZnSe}}-\varepsilon_{\text{eff}}(P)}{\varepsilon_{\text{ZnSe}}+2\varepsilon_{\text{eff}}(P)}=0,$$

where $\varepsilon_{\text{void}}=1$ is the dielectric constant of pores, $\varepsilon_{\text{ZnSe}}=9$ is the bulk value [39]. The value of ε_{eff} was obtained by numerically solving the equation iteratively in Matlab.

The electron affinity of porous ZnSe $\chi_{\text{eff}}(P)$ is related to the effective dielectric constant through the Penn relation, which describes the dependence of the work function on the shielding in the effective medium:

$$\chi_{\text{eff}}(P)=\chi_{\text{ZnSe}}-\alpha\left(1-\frac{\varepsilon_{\text{eff}}(P)}{\varepsilon_{\text{ZnSe}}}\right),$$

where $\alpha=1.0$ eV is the Penn parameter for II-VI semiconductors [40], $\chi_{\text{ZnSe}}=4.09$ eV is the electron affinity of bulk ZnSe [41]. The decrease in ε_{eff} with increasing porosity means a weakening of the shielding of electric fields in the material, which reduces the effective depth of the potential well for an electron and, accordingly, reduces the electron affinity.

The height of the potential barrier at the ZnO/porous-ZnSe interface is determined by the difference in electron affinities:

$$V_0(P)=\chi_{\text{ZnO}}-\chi_{\text{eff}}(P),$$

where $\chi_{\text{ZnO}}=4.35$ eV. The ZnO nanowire parameters are fixed throughout all calculations: effective electron mass $m^*=0.24\,m_0$. The effective mass is determined by the intrinsic band structure of ZnO and remains independent of the ZnSe substrate porosity. The barrier material parameters, which depend on the porosity of the ZnSe substrate, are summarized in Table 2.

As can be seen from Table 2, increasing the porosity from 0 to 80% increases V_0 from 0.26 eV (for bulk ZnSe) to 1.08 eV (for $P=80\%$). This means that porous ZnSe forms a significantly higher potential barrier than solid ZnSe, thereby enhancing the quantum confinement of the electron in the ZnO nanowire.

Finite cylindrical well model

In the finite cylindrical well model, the stationary Schrödinger equation is solved separately in two regions. Inside the ZnO nanowire ($r<R$), the potential is zero, and the solution for the ground state ($m=0$) is:

$$\psi(r)=A\,J_0(kr),\qquad k=\sqrt{\frac{2m^*_{\text{ZnO}}E}{\hbar^2}},$$

where J_0 is the Bessel function of the first kind of zero order (an oscillatory function describing the electron localization inside the nanowire). Outside the nanowire, in porous ZnSe ($r>R$), the potential equals $V_0(P)$, and the solution decays:

$$\psi(r)=B\,K_0(\kappa r),\qquad \kappa=\sqrt{\frac{2m^*_{\text{ZnSe}}(V_0-E)}{\hbar^2}},$$

where K_0 is a modified Bessel function of the second kind of zeroth order (a damping function describing the penetration of the wave function into the barrier layer). Since the thickness of the porous ZnSe layer significantly exceeds the radius of the nanowire, the wave function decays to zero within the porous layer, and the bulk ZnSe substrate does not affect the quantum states of the nanowire.

On the boundary $r=R$, the conditions of continuity of the wave function and its derivative

Table 2 – Parameters of the barrier material for the two heterostructure systems

Material	Porosity $P,\%$	Dielectric constant ε_{eff}	Potential $V_0(P)$, eV
ZnO/ZnSe(bulk)	0	9.00	0.260
ZnO/porous-ZnSe	20	6.77	0.508
ZnO/porous-ZnSe	40	4.66	0.742
ZnO/porous-ZnSe	60	2.87	0.941
ZnO/porous-ZnSe	80	1.64	1.078

are imposed, taking into account different effective masses in the two regions [32]:

$$\frac{k}{m^*_{\text{ZnO}}}\frac{J_1(kR)}{J_0(kR)} = \frac{\kappa}{m^*_{\text{ZnSe}}}\frac{K_1(\kappa R)}{K_0(\kappa R)},$$

where J_1 and K_1 are the firstorder Bessel functions of the first and second kind, respectively. This transcendental equation is solved numerically in Matlab by the bisection method for each value of the nanowire radius R and porosity P.

It should be noted that for low porosity values ($P < 20\%$) at large radii, or for high porosity values at $R > 15\,\text{nm}$, the condition for the existence of a bound state may not be fulfilled, which indicates that the barrier V_0 is insufficient to confine the electron in cylindrical geometry.

Therefore, the energy spectrum was calculated for the radius range $R = 5\ldots20\,\text{nm}$, where bound states exist for all considered porosity values. For bulk ZnSe ($P = 0\%$), the barrier height is only $V_0 = 0.26\,\text{eV}$, which represents a relatively weak confinement. With increasing porosity, the barrier increases to $V_0 = 1.08\,\text{eV}$ at $P = 80\%$, approaching the conditions of an infinite well.

Influence of porous ZnSe on the electronic states of ZnO nanowires

Numerical solution of the transcendental equation of a finite cylindrical well for the range of radii $R = 5\ldots20\,\text{nm}$ and porosity values $P = 0, 20, 40, 60, 80\%$ allowed us to establish the quantitative dependence of the ground state energy E_1 on the system parameters (Fig. 3).

As shown in Fig. 3, the ground-state energy follows the dependence $E_1 \propto 1/R^2$, which is characteristic of cylindrical quantum confinement. For all porosity values, increasing the nanowire radius leads to a reduction in E_1. It is important to note that within the finite potential well model, bound states do not exist for all combinations of R and P: for $P = 60\%$ and $P = 80\%$, the transcendental equation has no solution for $R > 16\,\text{nm}$ and $R > 15\,\text{nm}$, respectively. This is a physical consequence of the cylindrical geometry unlike the planar well, the cylindrical finite well requires a minimum barrier strength for a bound state to exist. Accordingly, the curves for high porosity values are shown only over the radius range where bound states are supported.

Comparison of the ZnO/ZnSe(bulk) and ZnO/porous-ZnSe/ZnSe structures confirms that porous ZnSe is a more effective substrate for the formation of pronounced quantum states.

The absolute shifts of the ground state $\Delta E_1 = E_1(P) - E_1(\text{bulk})$ are shown in Fig. 4. The largest effect is observed for thin nanowires ($R = 5\,\text{nm}$): the shift ranges from 2 meV at $P = 20\%$ to 3.7 meV at $P = 80\%$. With increasing radius, the shifts decrease, which is consistent with the decreasing role of quantum confinement in thick nanowires [42]. The physical reason for the shifts is that increasing porosity decreases $\varepsilon_{\text{eff}} \rightarrow$ decreases $\chi_{\text{eff}} \rightarrow$ increases $V_0 \rightarrow$ the wave function becomes more localized inside ZnO $\rightarrow$ the energy level shifts upward.

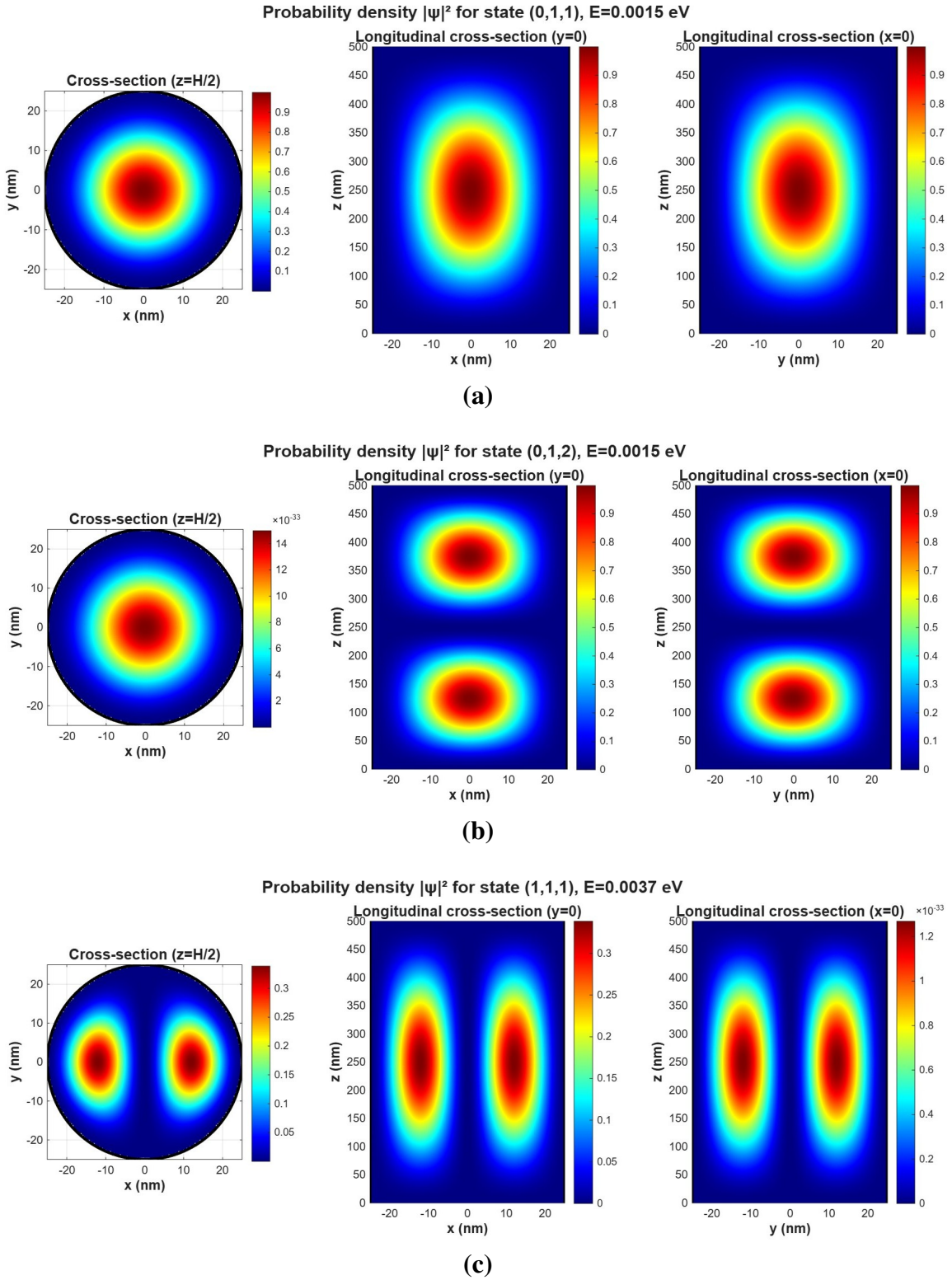

Figure 2 - Probability density distribution $|\psi|^2$ for three quantum states in a ZnO nanowire: (a) state $(0,1,1)$, (b) state $(0,1,2)$, (c) state $(1,1,1)$.

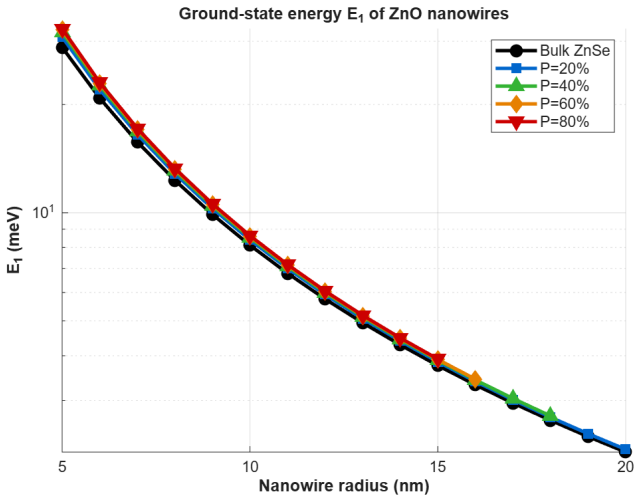

Figure 3 - Groundstate energy E_1 of ZnO nanowires as a function of radius for bulk ZnSe and porous ZnSe.

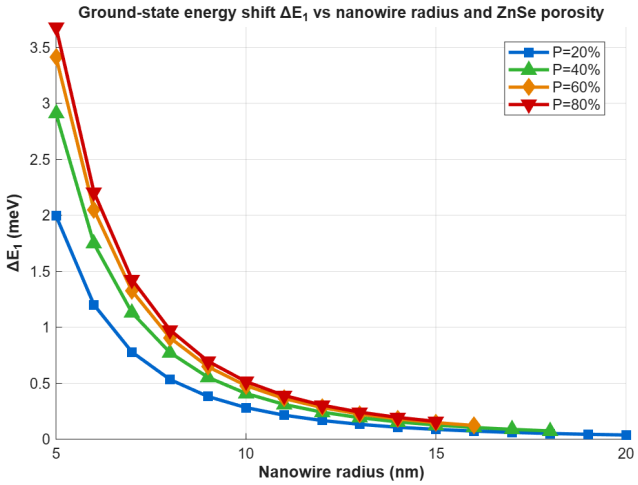

Figure 4 - Groundstate energy shift as a function of nanowire radius and ZnSe porosity.

Conclusions

The aim of this study was to theoretically determine the influence of a porous ZnSe layer on the formation of quantum states and electronic properties of ZnO nanowires in ZnO/ZnSe(bulk) and ZnO/porousZnSe/ZnSe heterostructures. To achieve this goal, a two-stage approach was used: an infinite cylindrical well model to describe the general structure of the energy spectrum, and a finite cylindrical well model to quantitatively analyze the effect of substrate porosity on quantum levels.

The results showed that radial quantum confinement dominates over longitudinal confinement, and the nanowire energy spectrum exhibits strong discreteness in the transverse direction and quasicontinuity along the axis.

It has been found that the porosity of ZnSe significantly changes the potential barrier at the ZnO/ZnSe interface: an increase in porosity from 0 to 80% increases the barrier height V_0 from 0.26 eV to 1.08 eV. This leads to a systematic shift of the energy levels: for nanowires with a radius of $R = 5$ nm, the absolute shift of the ground state ranges from 2 meV at $P = 20\%$ to 3.7 meV at $P = 80\%$. With an increase in the radius to $R = 20$ nm, the shifts decrease to submillielectronvolt values.

The novelty of the work lies in the combination of a self-consistent set of effective medium parameters (the Bruggeman equation for ε_{eff} and the Penn relation for χ_{eff}) with an analytical description of quantum confinement in a finite cylindrical well, which for the first time made it possible to obtain a quantitative model of the influence of ZnSe porosity on the energy spectrum of ZnO nanowires. The obtained results confirm the possibility of targeted control of quantum states by modifying the porosity of the substrate and open up prospects for the optimization of UV photodetectors, sensors, and photovoltaic converters.

Author Contributions: Conceptualization, A.D.; methodology, A.D.; data curation, A.D.; formal analysis, R.O.; resources, A.D.; software, E.F.; writing–original draft, A.D.; writing–review & editing, E.F.; visualization, R.O.; validation, R.O.; supervision, E.F.; funding acquisition, E.F.; project administration, R.O. All authors have read and agreed to the published version of the manuscript.

References

[1] Liu, S., W. Yang, L. Liu, H. Chen, and Y. Liu. "Enhanced H_2S gas-sensing performance of Ni-doped ZnO nanowire arrays." *ACS Omega* 8, no. 8 (2023): 7595–7601. https://doi.org/10.1021/acsomega.2c07092

[2] Wang, N., J. Li, C. Wang, X. Zhang, S. Ding, Z. Guo, and D. Jiang. "Improved UV photoresponse performance of ZnO nanowire array photodetector via effective Pt nanoparticle coupling." *Nanomaterials* 14, no. 17 (2024): 1442. https://doi.org/10.3390/nano14171442

[3] Xu, N., Z. Yuan, F. Nie, J. He, X. Wang, and S. You. "Hydrothermal growth and ultraviolet sensing performance of well-aligned Ga-doped ZnO nanowire arrays." *Optical Materials* 133 (2022): 112995. https://doi.org/10.1016/j.optmat.2022.112995

[4] Hyun, J. K., S. Zhang, and L. J. Lauhon. "Nanowire heterostructures." *Annual Review of Materials Research* 43, no. 1 (2013): 451–479. https://doi.org/10.1146/annurev-matsci-071312-121659

[5] Dhara, S. and P. K. Giri. "ZnO nanowire heterostructures: Intriguing photophysics and emerging applications." *Reviews in Nanoscience and Nanotechnology* 2, no. 3 (2013): 1–24. https://api.semanticscholar.org/CorpusID:54887802

[6] Hsu, H. C., C. S. Cheng, C. C. Chang, S. Yang, C. S. Chang, and W. F. Hsieh. "Orientation-enhanced growth and optical properties of ZnO nanowires grown on porous silicon substrates." *Nanotechnology* 16, no. 2 (2005): 297–301. https://doi.org/10.1088/0957-4484/16/2/021

[7] Irmer, G., E. Monaico, I. M. Tiginyanu, G. Gärtner, V. V. Ursaki, G. V. Kolibaba, and D. D. Nedeoglo. "Fröhlich vibrational modes in porous ZnSe studied by raman scattering and fourier transform infrared reflectance." *Journal of Physics D: Applied Physics* 42, no. 4 (2009): 045405. https://doi.org/10.1088/0022-3727/42/4/045405

[8] Monaico, E. *Morphology and Optical Properties of Porous Structures on the Basis of II–VI Semiconductor Compounds*. Chisinau: Moldova State University, 2009.

[9] Alamgeer, R., S. Hasan, S. A. U. Hasan, B. Zhao, H. Sadia, L. Siddiqui, and J. Yi. "Zinc oxide

nanostructures in photovoltaics: Recent progress, technical challenges and perspectives." *The Chemical Record* (2025): e2500142. https://doi.org/10.1002/tcr.202500142

[10] Dyadenchuk, A. F. and R. I. Oleksenko. "Simulation photoconverters of porous-Si/Si with different anti-reflective coatings." *International Journal of Mathematics and Physics* 14, no. 2 (2023): 89–94. https://doi.org/10.26577/ijmph.2023.v14.i2.010

[11] Clarke, B. and K. Ghandi. "The interplay of growth mechanism and properties of ZnO nanostructures for different applications." *Small* 19, no. 44 (2023): 2302864. https://doi.org/10.1002/smll.202302864

[12] Chen, Q., X. Liu, T. Wang, X. Su, M. Liu, S. Chaemchuen, and F. Verpoort. "A solvent-free process enabling ZnO/porous carbon with enhanced microwave absorption." *Journal of Materials Science & Technology* 149 (2023): 255–264. https://doi.org/10.1016/j.jmst.2022.12.034

[13] Lebib, A., L. Beji, and N. Hamdaoui. "Investigation of n-ZnO/p-porous GaAs/p++-GaAs heterostructure for photodetection applications." *Optical and Quantum Electronics* 56, no. 4 (2024): 660. https://doi.org/10.1007/s11082-023-06256-9

[14] Rong, X., F. Qiu, Z. Jiang, J. Rong, J. Pan, T. Zhang, and D. Yang. "Preparation of ternary combined ZnO-Ag_2O/porous g-C_3N_4 composite photocatalyst and enhanced visible-light photocatalytic activity for degradation of ciprofloxacin." *Chemical Engineering Research and Design* 111 (2016): 253–261. https://doi.org/10.1016/j.cherd.2016.05.010

[15] Khudiar, S. S., U. M. Nayef, F. A. H. Mutlak, and S. K. Abdulridha. "Characterization of NO_2 gas sensing for ZnO nanostructure grown hydrothermally on porous silicon." *Optik* 249 (2022): 168300. https://doi.org/10.1016/j.ijleo.2021.168300

[16] Morales-Morales, F., A. Benítez-Lara, N. Hernández-Sebastián, F. Ambriz-Vargas, M. R. Jiménez-Vivanco, R. López, and A. Morales-Sánchez. "Study of zinc oxide/porous silicon interface for optoelectronic devices." *Materials Science in Semiconductor Processing* 148 (2022): 106810. https://doi.org/10.1016/j.mssp.2022.106810

[17] Singh, R. G., F. Singh, V. Agarwal, and R. M. Mehra. "Photoluminescence studies of ZnO/porous silicon nanocomposites." *Journal of Physics D: Applied Physics* 40, no. 10 (2007): 3090. https://doi.org/10.1088/0022-3727/40/10/012

[18] Dyadenchuk, A., R. Oleksenko, and Y. Kuris. "Structural and electrical characteristics of the ZnO/porous-Si/Si heterostructure: From synthesis to analysis of photocell efficiency." *International Journal of Mathematics and Physics* 15, no. 2 (2024): 34–41. https://doi.org/10.26577/ijmph.2024v15i2b4

[19] Bouzourâa, M. B., A. E. Naciri, A. Moadhen, H. Rinnert, M. Guendouz, Y. Battie, and M. Oueslati. "Effects of silicon porosity on physical properties of ZnO films." *Materials Chemistry and Physics* 175 (2016): 233–240. https://doi.org/10.1016/j.matchemphys.2016.03.026

[20] Dyadenchuk, A., N. Domina, and R. Oleksenko, "Simulation of solar element characteristics based on porous silicon." in *2022 IEEE 4th International Conference on Modern Electrical and Energy Systems (MEES)*. Piscataway: IEEE, 2022, 1–4. https://doi.org/10.1109/MEES58014.2022.10005773

[21] Perumal, R., L. Saravanan, and J. H. Liu. "Substrate and doping effects on the growth aspects of zinc oxide thin films developed on a GaN substrate by the sputtering technique." *Processes* 13, no. 4 (2025): 1257. https://doi.org/10.3390/pr13041257

[22] Aspoukeh, P. K., A. A. Barzinjy, and S. M. Hamad. "Synthesis, properties and uses of ZnO nanorods: A mini review." *International Nano Letters* 12, no. 2 (2022): 153–168. https://doi.org/10.1007/s40089-021-00349-7

[23] Vlassov, S., D. Bocharov, B. Polyakov, M. Vahtrus, A. Šutka, S. Oras, and A. Kyritsakis. "Critical review on experimental and theoretical studies of elastic properties of wurtzite structured ZnO nanowires." *Nanotechnology Reviews* 12, no. 1 (2023): 20220505. https://doi.org/10.1515/ntrev-2022-0505

[24] Hadia, N. M. A., M. Alzaid, B. Alqahtani, M. Al-Shaghdali, W. S. Mohamed, M. Ezzeldien, and M. A. Awad. "Enhancement of optical, electrical and sensing characteristics of ZnO nanowires for optoelectronic applications." *Journal of Materials Science: Materials in Electronics* 34, no. 5 (2023): 456. https://doi.org/10.1007/s10854-023-09905-7

[25] Goswami, N., N. Tabassum, M. R. Habib, and M. Kabiruzzaman. "Analysis of electron confinement in semiconductor (Ge, GaN, and ZnO) quantum nanowires." *Evergreen* 12, no. 1 (2025): 18–26. https://api.semanticscholar.org/CorpusID:277603874

[26] Ursaki, V. V., V. V. Zalamai, A. Burlacu, C. Klingshirn, E. Monaico, and I. M. Tiginyanu. "Random lasing in nanostructured ZnO produced from bulk ZnSe." *Semiconductor Science*

and Technology 24, no. 8 (2009): 085017. https://doi.org/10.1088/0268-1242/24/8/085017

[27] Dyadenchuk, A. F. and V. V. Kidalov. "Production of porous ZnSe by electrochemical etching method." *Journal of Nano & Electronic Physics* 5, no. 3 (2013): 03033.

[28] Monaico, E., P. Tighineanu, S. Langa, H. L. Hartnagel, and I. Tiginyanu. "ZnSe based conductive nanotemplates for nanofabrication." *Physica Status Solidi (RRL) – Rapid Research Letters* 3, no. 4 (2009): 97–99. https://doi.org/10.1002/pssr.200903026

[29] Paul, R. K., S. Roy, and M. Ahmaruzzaman. "Zinc selenide engineered nanostructures: Insights into modification strategies, and multifunctional applications in environmental remediation, gas sensing, energy storage, and antimicrobial activity." *RSC Advances* 15, no. 58 (2025): 50 270–50 323. https://doi.org/10.1039/D5RA07718D

[30] Wu, X., R. Xu, R. Zhu, R. Wu, and B. Zhang. "Converting 2D inorganic–organic ZnSe–DETA hybrid nanosheets into 3D hierarchical nanosheet based ZnSe microspheres with enhanced visible light driven photocatalytic performances." *Nanoscale* 7, no. 21 (2015): 9752–9759. https://doi.org/10.1039/C5NR02329G

[31] Kidalov, V., N. Sosnytska, A. Dyadenchuk, and R. Oleksenko. "ZnO nanowires for photoelectric converter applications." *International Journal of Mathematics and Physics* 12, no. 2 (2021): 70–78. https://doi.org/10.26577/ijmph.2021.v12.i2.08

[32] Feit, M. D., J. A. Fleck Jr, and A. Steiger. "Solution of the schrödinger equation by a spectral method." *Journal of Computational Physics* 47, no. 3 (1982): 412–433. https://doi.org/10.1016/0021-9991(82)90091-2

[33] Sosnytska, N., A. Dyadenchuk, M. Morozov, and L. Khalanchuk, "Modeling of solar cells with quantum dots GaN." in *2021 IEEE International Conference on Modern Electrical and Energy Systems (MEES)*. Piscataway: IEEE, 2021, 1–5. https://doi.org/10.1109/MEES52427.2021.9598662

[34] Bowman, F. *Introduction to Bessel Functions*. New York: Dover, 1958.

[35] Sze, S. M., Y. Li, and K. K. Ng. *Physics of Semiconductor Devices*. Hoboken: John Wiley & Sons, 2021.

[36] Arbiol, J. and Q. Xiong, Eds. *Semiconductor Nanowires: Materials, Synthesis, Characterization and Applications*. Amsterdam: Elsevier, 2015. https://doi.org/10.1016/C2013-0-16507-5

[37] Lundstrom, M. S. *Fundamentals of Nanotransistors*. Singapore: World Scientific Publishing Company, 2017, 6. https://doi.org/10.1142/9018

[38] Zhang, D., E. Cherkaev, and M. P. Lamoureux. "Stieltjes representation of the 3D bruggeman effective medium and padé approximation." *Applied Mathematics and Computation* 217, no. 17 (2011): 7092–7107. https://doi.org/10.1016/j.amc.2011.01.020

[39] Adachi, S. *Properties of Group-IV, III-V and II-VI Semiconductors*. Hoboken: John Wiley & Sons, 2005. https://doi.org/10.1002/0470090340

[40] Cirilo-Lombardo, D. J. "Semiconductor dielectric function, excitons and the penn model." *Philosophical Magazine* 95, no. 9 (2015): 1007–1015. https://doi.org/10.1080/14786435.2015.1015468

[41] Sze, S. M. and K. K. Ng. "Leds and lasers."*In* , 601–657. Wiley, 2006. https://doi.org/10.1002/9780470068328.ch12

[42] Harrison, P. and A. Valavanis. *Quantum Wells, Wires and Dots: Theoretical and Computational Physics of Semiconductor Nanostructures*. Hoboken: John Wiley & Sons, 2016. https://doi.org/10.1002/9781118923337

Information about authors

Alena Dyadenchuk *– PhD, Associate Professor, Department of Higher Mathematics and Physics, Dmytro Motornyi Tavria State Agrotechnological University, Melitopol, Ukraine, e-mail: alena.dyadenchuk@tsatu.edu.ua*

Roman Oleksenko *– Doctor of Science, Professor, Volodymyr Vynnychenko Central Ukrainian State University, Kropyvnytskyi, Ukraine, e-mail: roman.xdsl@ukr.net*

Yevhenii Filipovych *– Masters student, Dmytro Motornyi Tavria State Agrotechnological University, Melitopol, Ukraine, e-mail: zhenyaq234@gmail.com*